Short Fiber-Reinforced Thermoplastic Elastomers from Blends of Natural Rubber and Polyethylene

S. AKHTAR, P. P. DE, and S. K. DE, *Rubber Technology Centre, Indian Institute of Technology, Kharagpur 721302, India*

Synopsis

Thermoplastic elastomer blends of natural rubber (NR) with high density polyethylene (HDPE) and with low density polyethylene (LDPE) were reinforced with short silk fiber. Processing characteristics such as torque and temperature developed during mixing and the effect of processing parameters such as nip gap and number of passes in the mill necessary to secure maximum orientation of the fibers in the blends were studied. A small nip gap and a single pass in the mill were found to give best results. Of the different mixing sequences studied, the sequence where short fibers followed by rubber were added to the molten thermoplastic was found to give a uniform dispersion of fibers. Fiber breakage and the change in aspect ratio of the fibers after mixing were also examined. It was observed that, as a direct consequence of the mixing sequence, each fiber was coated with a layer of thermoplastic. Although the properties improved on the addition of the dry bonding system of silica–resorcinol–hexamethylenetetramine, the comparatively long curing time required for full development of adhesion between the fibers and the matrix proved to be a major disadvantage associated with the incorporation of the bonding system. The tensile and tear properties were substantially enhanced, but the ultimate elongation decreased sharply with increasing loading of short fibers in the blends. The effect of fiber orientation and the development of anisotropy in the properties was also noted. Scanning electron microscopy (SEM) studies of the benzene-extracted surfaces of the NR/HDPE (high density polyethylene) blends substantiated the theory of fibers behaving like "mechanical anchors" between the rubber and thermoplastic phase. The effect of fiber loading on the tear and tensile properties of the blends of NR/LDPE with varying blend ratios was studied. Most pronounced improvement in the properties on the addition of short fibers was observed in the high rubber blends. As the plastic content in the blends increased, the short fibers were found to have a lesser influence on the properties. SEM photomicrographs of the tensile and tear fracture surfaces indicated the fiber orientations and the effect of orientation, fiber loading, and blend ratios on the nature of fracture.

INTRODUCTION

Over the last decade, short-fiber reinforcement of rubber has gained considerable attention as a viable alternative to particulate filler reinforcement because of the typical advantages associated with fibrous fillers which include design flexibility, high low strain moduli, anisotropy in technical properties, stiffness, damping, and processing economy. Short-fiber-reinforced elastomers have been successfully used in the production of hoses, V-belts, tyre treads, seals, and complex-shaped mechanical goods. The extent of reinforcement is found to depend on the fiber–matrix adhesion, aspect ratio of the fiber in the vulcanizate, fiber dispersion and orientation, nature of matrix, and type of fiber.[1–5]

Journal of Applied Polymer Science, Vol. 32, 5123–5146 (1986)
 CCC 0021-8995/86/055123-24$04.00

While different types of continuous fibers have earlier[6–10] been used to reinforce thermoplastics, some investigations have been reported[11] on the use of discontinuous fibers in thermoplastics. However, so far as thermoplastic elastomers are concerned, no reference is available on the usage of a fibrous filler.

In the present paper, we report the results of our investigations on short silk fiber reinforcement of thermoplastic elastomer blends composed of natural rubber (NR) and polyethylene (PE), both high and low density varieties. In an earlier paper[12] we have characterized the NR/PE blends. In this paper we have used short silk fiber, obtained as waste during cocoon reeling, which is unusable as such in the textile industry. In this context, the present work deals with the utilization of a waste material. Setua and De[13–15] have reported their results on the short silk fiber reinforcement of various rubber vulcanizates. Our preliminary studies on short-fiber-filled NR/PE blends indicated a twofold increment in the tensile strength and a threefold increment in the tear strength at 20 phr fiber loading in the high rubber blends with longitudinal fiber orientation. Following it up, we have investigated in details the processing characteristics and mechanical properties and the effects of (1) blend ratio, (2) fiber loading, (3) processing conditions, and (4) fiber orientation on these properties. Fiber breakage and the corresponding change in aspect ratio have also been reported.

The improvement in reinforcement obtained by enhancing fiber–matrix adhesion through the incorporation of a bonding system has been widely studied in the case of rubber vulcanizates.[16–18] We have also sought to examine, in this paper, the role played by a bonding system in the case of short-fiber-filled NR/PE blends. For this purpose, we have chosen the tricomponent dry bonding system composed of silica, resorcinol, and hexamethylenetetramine.

Finally, we have made scanning electron microscopic (SEM) studies of the tensile and tear failed specimen surfaces in order to understand the failure mechanism of the blends in the presence of short fibers.

MATERIALS

Natural Rubber (NR). Crumb rubber, ISNR 5 grade: obtained from the Rubber Research Institute of India, Kottayam. Density = 0.920 g/cm^3.

High Density Polyethylene (HDPE). HOSTALEN GA 7260: obtained from Polyolefins Industries Ltd., Bombay. Density = 0.960 g/cm^3; MFI = 52 g/10 min; crystalline melting range = 128–132°C.

Low Density Polyethylene (LDPE). INDOTHENE 16 MA 400: obtained from Indian Petrochemicals Corporation Ltd., Vadodara. Density = 0.916 g/cm^3; MFI = 40 g/10 min; crystalline melting point = 110–112°C.

Silk Fiber. Waste silk fiber (mulberry type) was supplied by the Silk Khadi Mondal, Bishnupur. It was first separated from undesirable foreign matter and then chopped to 6.0 mm length. Average fiber filament diameter = 0.0045 mm.

Silica. Vulcasil-S was obtained from Bata India Ltd., Calcutta.

Hexamethylenetetramine (Hexa) was supplied by May and Baker, England.

TABLE I
Formulations of the Mixes[a]

Ingredients	A	B	C	D
NR	30	50	70	70
LDPE	70	50	30	—
HDPE	—	—	—	30

[a] Fibre loadings were based on the rubber phase only and are indicated by the number prefixing the mix: e.g., 0C, 5C, 10C, etc., where 0, 5, and 10 denote the fibre loading (phr) in mix C (70 NR/30 LDPE).

EXPERIMENTAL

Formulations of the mixes are given in Table I. Fiber-filled blends of NR/LDPE and NR/HDPE were prepared in a Brabender Plasticorder (Model PLE 330), using a cam-type mixer with a rotor speed of 60 rpm and the mixer chamber temperature set at 150°C. Different mixing sequences were tried out and the dispersion of fibers was observed in each case (as shown in Table II). Thus, the best mixes were obtained when the polyethylene was melted in the mixer for 2 min, chopped silk fiber was added to it, and it was mixed for another 2 min. This was followed by the addition of NR, which was mixed for 4 min. The mix was then taken out and sheeted through a laboratory mill at an optimum nip setting. The sheeted material was then remixed in the plasticorder at 150°C for 2 min and finally sheeted out on a steam-heated mill (temperature = 85 ± 5°C). The latter step was necessary to secure proper orientation of the fibers in the mix. Shear forces during milling oriented most of the fibers in the grain direction. The sheeted out stock was compression-molded between aluminium foils in an electrically heated hydraulic press at 150°C for 3 min. The mold used was provided with bolts and nuts so that the material inside could be held under pressure even after taking the mold out of the press. At the end of the molding time, the sample, still under compression, was immediately cooled by plunging the mold into cold water. Aluminium foils were used between the mold surfaces to reduce shrink marks on the sheets. The non-fiber-filled blends were also prepared by the same method.

TABLE II
Mixing Sequence and Dispersion of Fibers

Mixing sequence	Dispersion of fibers
1. Molten thermoplastic + rubber + short fiber	Poor; fibers are not properly incorporated
2. Rubber + short fiber + thermoplastic	Poor; fibers lump together and a nonuniform dispersion results
3. Molten thermoplastic + part of short fiber loading + rubber + part of short fiber loading.	Intermediate; fewer lumps and more uniform dispersion of fibers
4. Molten thermoplastic + short fiber + rubber	Good; uniform dispersion of fibers

In the cases, where bonding system was incorporated, a masterbatch of NR and the bonding system was first prepared at 60°C. NR was masticated in the Brabender at 60°C, and then silica was added to it and mixed; this was followed by the addition of premelted resorcinol. Finally, hexamethylenetetramine was added and mixed. This masterbatch was added to the polyethylene and fiber as previously mentioned and mixed, taking care to maintain proper viscosity levels. The measurement of the length distribution of the short fibers was made by refluxing the molded sheet of the short-fiber-filled NR/LDPE blend in benzene to dissolve the matrix. The lengths of the separated fibers were then measured using an optical microscope. From the results, the change in fiber length distribution during the mixing process was obtained. Tensile testing of the samples (thickness = 2 ± 0.2 mm) was done at 25°C as per ASTM D412-80 test method using dumbbell-shaped test pieces cut along (L = longitudinal fiber orientation) and across (T = transverse fiber orientation) the mill grain directions, at a crosshead speed of 500 mm per min, using an Instron Universal testing machine, Model 1195. Tear strength of the samples was determined as per ASTM D624-81 test method using unnicked 90° angle test pieces punched out along and across the mill grain direction from the molded sheets. Figures 1 and 2 show

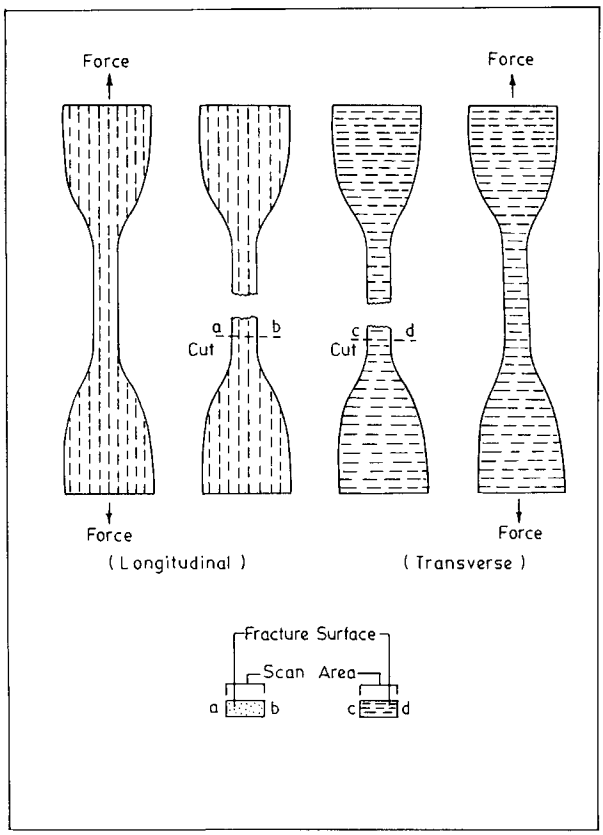

Fig. 1. Shape of tensile test specimen, direction of fiber orientation, fracture surface, and SEM scan area.

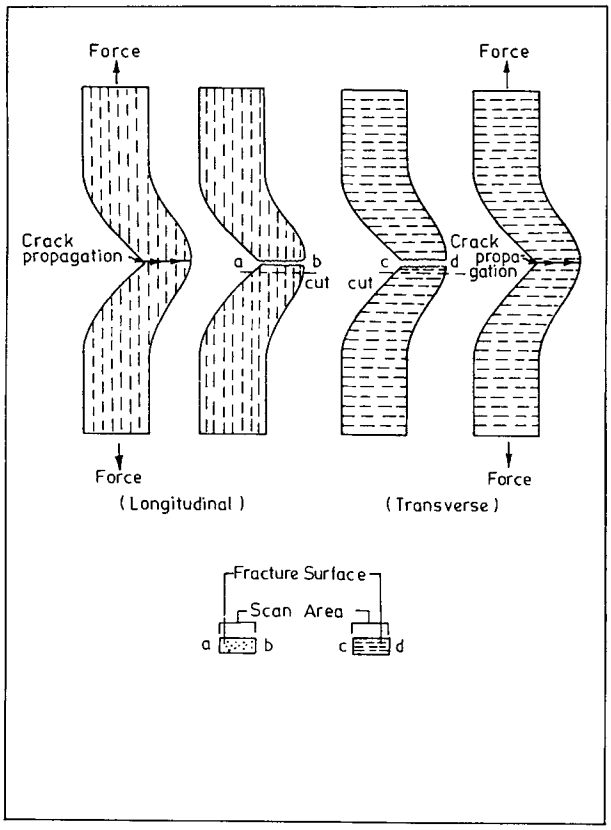

Fig. 2. Shape of tear test specimen, direction of fiber orientation, fracture surface, and SEM scan area.

the tensile and tear test specimens respectively and the direction of fiber orientation.

The SEM observations of the tensile failure surfaces of short-fiber-filled NR/LDPE blends and of the benzene-extracted surfaces of NR/HDPE blends were made using a Philips scanning electron microscope, Model 500. The tilt was kept at 0°, and the orientation of the photographs was kept the same in all cases.

RESULTS AND DISCUSSION

The results have been divided into two parts:

1. Effect of fiber loading on the processing and physical properties of NR/LDPE and NR/HDPE fiber-filled composites having the composition 70 pbw rubber/30 pbw thermoplastic, SEM studies of the benzene extracted surface.

2. Effect of fibre loading on the mechanical properties of NR/LDPE fiber-filled blends with varying blend ratio; SEM studies of the tensile and tear fracture surfaces of the different blends.

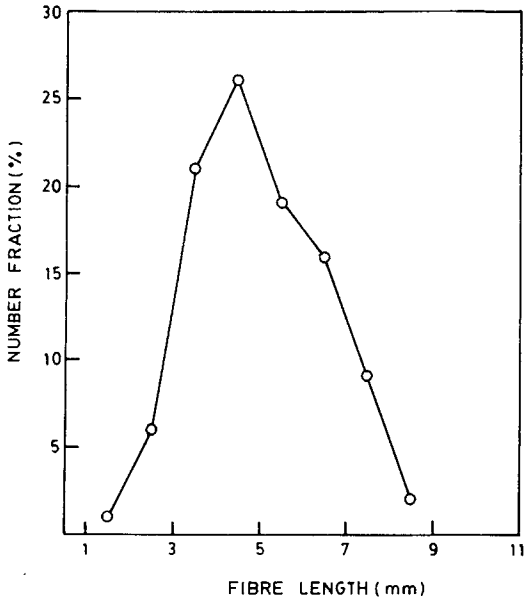

Fig. 3. Fiber length distribution: maximum distribution occurs at 4.5 mm.

PART I

Fiber Breakage. The breakage of the short fibers during the milling process depends on the type of fiber, their length and diameter, and the level of adhesion between the fiber and the blend matrix. We studied the breakage of fibers in short-fiber-filled NR–LDPE blend; fiber loading = 30 phr (parts per hundred rubber). It was observed that the short silk fibers exhibited a series of bends and kinks after mixing which resulted in breakage. On the other hand, since each fiber was made up of several filaments, many fibers split into filaments (of smaller diameter) during mixing.

Figure 3 shows the fiber length distribution after mixing. The maximum

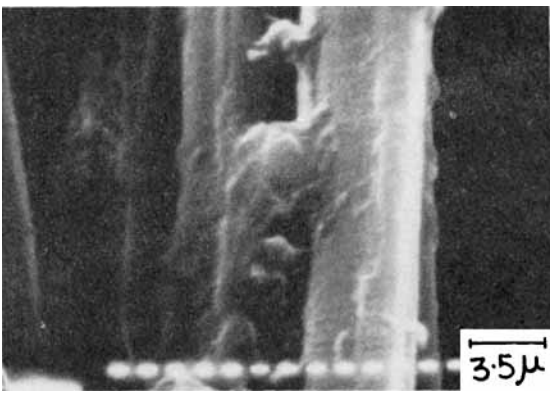

Fig. 4. Coating of thermoplastic material on the fiber extracted with benzene from the blend.

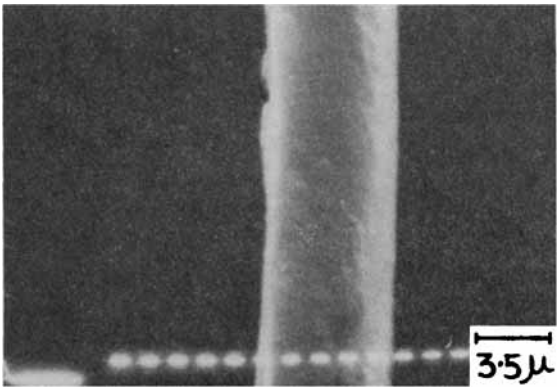

Fig. 5. Fiber filament before mixing.

distribution occurs at about 4.5 mm indicating a moderate amount of breakage of the fibers during mixing. It was also observed (Fig. 4) that the fibers had a coating of the plastic material which was formed as a direct consequence of the addition of the fibers to the molten thermoplastic as per the mixing sequence. Consequently, the average diameter of the fiber filament appeared to increase from 0.0045 to 0.0051 mm as shown in Figures 5 and 6, which are the SEM photomicrographs of the filament before mixing and after mixing and extraction respectively.

The aspect ratio (length to diameter) of the fibers changes from 1333 before mixing to 1000 after mixing, although if the apparent increase in the diameter of the fiber is taken into account, it becomes 882 after mixing.

Processing Characteristics

Mixing characteristics of the fiber-filled NR–LDPE and NR–HDPE composites are given in Table III. The torque increases with increasing fiber loading. Frictioning between the fibers and the matrix leads to an increase in the stock temperature which is found to increase with increasing fiber

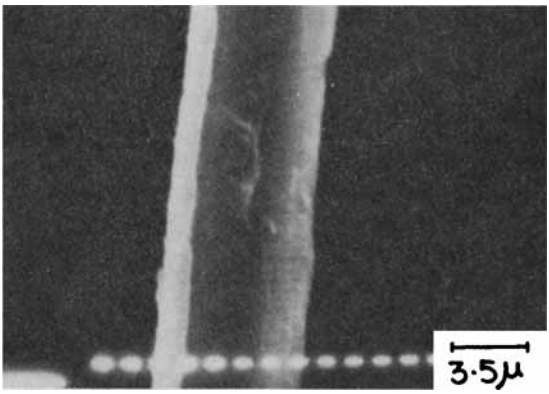

Fig. 6. Fiber filament extracted with benzene from the blend: increase in diameter due to coating of thermoplastic.

TABLE III
Mixing Characteristics of Short Fiber Filled NR–PE Blends

Mix no.	30C						30D				
Fiber loading (phr)	0	5	10	20	30	40	0	10	20	30	40
Mixing torque after 8 min (N/m)	7	11	13	18	19	24	7.5	21	23	25	28
Stock temperature (°C)	153	157	158	160	161	167	155	155	156	156	159

concentration in the blends. HDPE composites show higher mixing torque than the corresponding LDPE ones.

We have studied the effect of processing conditions such as nip gap of the mill and number of passes in the mill on the final properties of the fiber-filled composites. The variation of tensile properties of mixes 30C (30 LDPE/70NR/30 fiber) and 30D (30 HDPE/70NR/30 fiber) were studied against a varying nip gap. It was observed (Table IV) that tensile strength and anisotropy in physical properties in the composites decreased with increase in the nip gap. But no clear trend was observed in the tear strength values. It can be concluded from Table IV that, as in the case of short-fiber-filled rubber vulcanizates,[19] the nip gap does not have too pronounced an effect on the strength properties but a small nip gap leads to better orientation of the fibers and hence to higher anisotropy and tensile properties. We chose a nip gap of 1.25 mm for further studies.

The effect of number of passes on the tensile and tear strengths of mixes 30C and 30D are given in Table V. The tensile strength is highest after one pass only but the tear strength varies arbitrarily with the number of passes in the mill. It is very likely that most of the fibers get oriented in the first pass itself and any further passes through the mill have a randomizing effect on the orientation. More than one pass, therefore, does not appear necessary so far as the orientation of the fibers along the mill direction in a thermoplastic elastomer is concerned. Similar observations have been made in the case of short-fiber-filled rubber vulcanizates.[19]

TABLE IV
Effect of Nip Gap on the Physical Properties of the Composites

Mix no.		30C				30D			
Nip gap (mm)		0.80	1.25	2.20	3.30	0.90	1.25	1.75	3.00
Tensile strength (MPa)	L	13.2	14.9	11.5	11.9	11.7	19.1	13.8	14.0
	T	3.9	4.3	5.0	5.4	4.4	4.1	8.6	7.9
Elongation at break (%)	L	50	45	50	50	220	160	200	190
	T	170	130	95	100	250	200	190	250
Tear strength (kN/m)	L	54.5	46.5	44.8	51.2	66.8	82.6	66.7	81.6
	T	30.0	31.3	33.1	31.5	36.6	39.2	65.1	52.8

TABLE V
Effect of Number of Passes on the Physical Properties of Composites

Mix no.		30C				30D			
Number of passes		1	3	5	7	1	3	5	7
Tensile strength	L	14.9	14.0	9.3	13.4	15.3	12.8	12.3	12.4
(MPa)	T	4.3	4.5	4.8	4.9	6.1	5.7	5.2	4.9
Elongation at	L	45	40	50	60	180	200	185	120
break (%)	T	130	125	130	55	440	440	490	550
Tear strength	L	46.5	42.0	47.5	45.0	72.1	91.6	69.2	77.5
(kN/m)	T	31.6	32.0	26.7	31.0	44.2	64.2	49.2	37.2

Effect of Bonding System

The dry bonding system, consisting of silica, resorcinol, and hexamethylenetetramine, was added to the high rubber blend containing 3 phr fiber in order to improve the adhesion between the fibers and the blend matrix. While both tensile and tear strengths showed significant enhancement, the elongation at break values dropped considerably in both fiber orientations (Table VI). By increasing the total amount of the bonding system (added in the same proportion and sequence), further improvements were noted in the tensile and tear results except at very high loadings.

Choosing a particular proportion of the bonding system, we studied the effect of cure time of the bonding system on the properties of the mixes (Table VII). It was observed that, as the cure time increased, the properties improved. On the other hand, one of the major advantages of thermoplastic elastomers is their easy processing and molding and elimination of the vulcanization step. Normally, after blending, molding takes about 2 min for a thermoplastic elastomer, whereas, on the addition of a bonding agent, an additional molding time of 10 min or more is necessary for attaining a significant level of adhesion. Thus, the cure time of the bonding system negates the advantages associated with thermoplastic elastomers, and hence

TABLE VI
Effect of Proportion of Bonding System on Physical Properties of the Composites

Mix no.		30C					30D				
Bonding system		0	1	2	3	4	0	1	2	3	4
Silica		—	2.5	5	7.5	10	—	2.5	5	7.5	10
Resorcinol		—	12.5	2.5	3.75	5	—	1.25	2.5	3.75	5
Hexamethylene-tetramine		—	0.8	1.6	2.4	3.2	—	0.8	1.6	2.4	3.2
Tensile strength	L	14.9	16.6	16.6	15.4	12.4	15.7	15.8	17.2	19.2	15.6
(MPa)	T	4.2	4.8	5.9	5.9	6.5	5.9	6.1	7.3	5.6	6.1
Elongation at	L	45	22	30	36	50	210	225	90	100	180
break (%)	T	130	90	70	70	80	290	190	320	176	440
Tear strength	L	43.4	60.8	58.7	63.4	65.7	86.4	75.1	91.1	93.1	72.1
(kN/m)	T	33.1	36.0	41.7	44.1	38.0	49.7	57.6	61.8	50.0	44.2

TABLE VII
Effect of Curing Time of Bonding System on Physical Properties of Composites

Mix no.		30C[a]					30D[a]				
Time (min)		3	5	10	15	20	3	5	10	15	20
Tensile strength (MPa)	L	—	14.5	16.5	18.2	19.1	—	13.4	15.1	14.7	17.0
	T	—	5.7	5.7	5.9	6.1	—	5.8	5.7	5.6	5.6
Elongation at break (%)	L	—	30	30	20	25	—	275	150	80	160
	T	—	85	80	70	70	—	400	560	400	200
Tear strength (kN/m)	L	—	59.8	59.8	64.3	63.8	—	67.3	69.9	73.5	55.2
	T	—	39.8	43.1	41.0	41.6	—	52.9	51.8	34.5	45.3

[a] Bonding system: silica 5; resorcinol 2.5; hexamethylenetetramine 1.6.

we did not consider it worthwhile to pursue studies on the usage of a bonding system in such composites.

Physical Properties

Figure 7 shows the variation of tensile strength of the NR/PE blends with increasing fiber loading. The tensile strength increases continuously except at low fiber loadings where there appears to be a decrease. This decrease has been explained by many researchers[20,21]: at low concentrations the matrix is not restrained by enough fibers and high localized strains occur in the matrix at low stresses, causing the bond between fiber and rubber to break, leaving the matrix diluted by nonreinforcing, debonded fibers. As the fiber concentration increases, the matrix is restrained and the stress more evenly distributed. It is also clear from Figure 7 that the inclusion of

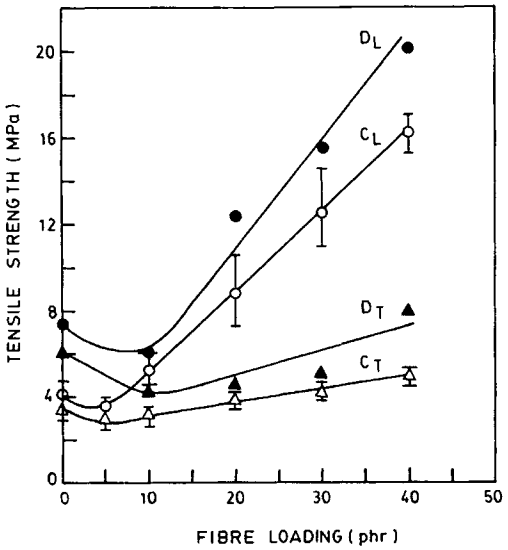

Fig. 7. Plot of tensile strength vs. fiber loading for the NR/LDPE (C_L and C_T) and NR/HDPE (D_L and D_T) blends.

fiber in the mixes leads to anisotropy, depending on the direction and degree of fiber orientation. At any given fiber loading, mixes with longitudinal fiber orientation show higher tensile strength than mixes with transverse fiber orientation. It was observed that while the tensile strength increases rapidly with increase in fiber loading in the longitudinal direction, in the transverse direction the increase is less pronounced. HDPE blends show consistently higher values in all cases as compared to the LDPE blends (Fig. 7). The "dilution effect" is pronounced at 5 phr in LDPE composites and at 10 phr in HDPE composites.

Figure 8 shows the effect of fiber loading on the modulus (at 25% elongation). The modulus increases slowly at low loadings of fiber but after about 10 phr loading of fiber it increases rapidly. Modular anisotropy is observable, at 25% elongation. When the fibers are aligned across the direction of application of force (i.e., transverse fiber orientation), they do not contribute much to the modulus of the matrix, but when they are oriented along the direction of application of stress (i.e., longitudinal fiber orientation), they act in conjunction with matrix in increasing the modulus of the composite.[14]

The ultimate elongation of the blends undergoes a sharp fall on the introduction of fibers in the mixes (Fig. 9). But with increase in fiber loading

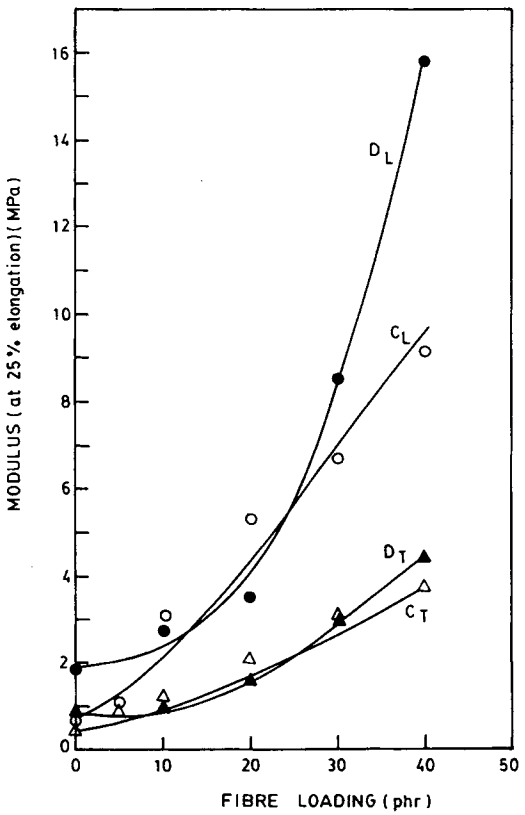

Fig. 8. Plot of modulus at 25% elongation vs. fiber loading for the NR/PE blends.

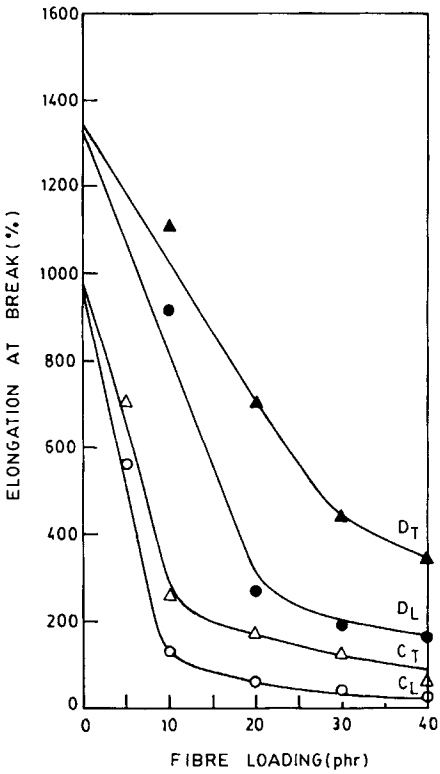

Fig. 9. Plot of elongation at break vs. fiber loading for the NR/PE blends.

the elongation at break decreases much more gradually in contrast to the initial drop. The elongation at break values of the blends with longitudinally oriented fibers drop drastically up to a loading of 10 phr, beyond which the drop becomes gradual. In the case of mixes with transversely oriented fibers, the trend remains the same, but higher values are observed in all cases. The fibers inhibit the orientation of the molecular chains and hence the ultimate elongation decreases substantially on the introduction of fibers in the mixes. From the variation of tensile strength and elongation at break values, it is clear that the role of fiber as a reinforcing filler is evident only when the fiber concentration exceeds 10 phr.

Tear strength follows the same trend as tensile strength and is significantly enhanced in the presence of short fibers in all the blends (Fig. 10) as it is in the case of silk-fiber-filled rubber vulcanizates.[12–14]

The concept of anisotropy is amplified in the trend exhibited by both the fiber-filled blends: the tear strength increases slowly in the case of mixes with transverse fiber orientation and levels off at about 30 phr loading of fiber unlike in mixes with longitudinal fiber orientation. In the case of longitudinally oriented fibers, the matrix get deformed while the fibers inhibit the propagating fracture path. In the case of transversely oriented fibers, the crack progresses in the direction of fiber alignment and tensile strength in this direction is less than that in the case of longitudinally

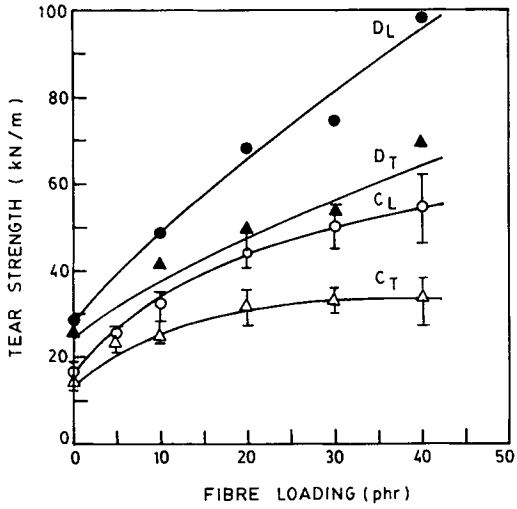

Fig. 10. Plot of tear strength vs. fiber loading for the NR/PE blends.

oriented fibers, where the crack progresses perpendicularly to the fiber orientation direction.

SEM Studies of Extracted Surfaces

On quantitative extraction of the rubber phase with benzene, the high rubber blend (70 NR/30 HDPE) was found to split into several layers. Figures 11 and 12 show the SEM photomicrographs of the surface of one of the layers formed after extraction of the blend by benzene. Only HDPE blends were extracted with benzene and not the LDPE blends because the rubber phase could not be selectively extracted from the latter. From these figures it appears that the thermoplastic component forms a continuous phase despite the fact that in this blend the rubber content is comparatively much higher. This is possibly due to the low viscosity of HDPE. Figure 13 is the corre-

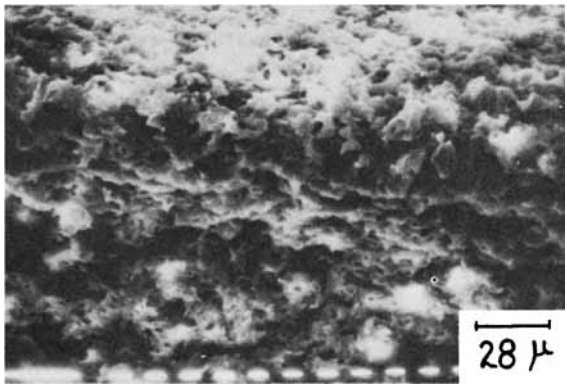

Fig. 11. SEM photomicrograph of benzene extracted surface of blend D (70 NR/30 HDPE): HDPE also forms a continuous phase.

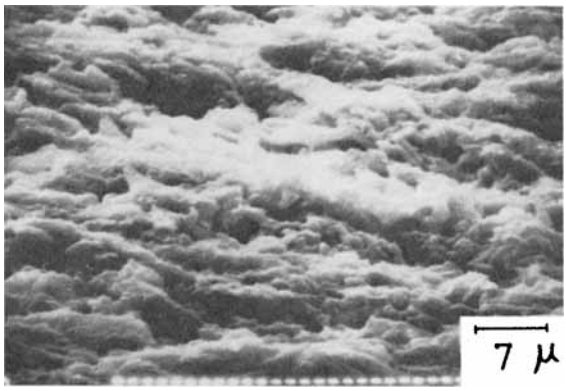

Fig. 12. SEM photomicrograph of benzene extracted surface of blend D: enlarged view of Figure 11.

sponding photomicrograph of the blend filled with 30 phr of short silk fiber. The characteristics of this surface are much different from those of the unfilled blend (Figs. 11 and 12), although the thermoplastic phase is continuous in nature as in the case of unfilled blends. In the case of fiber-filled blends, on extraction with benzene, several fiber ends stick out of the layer (Fig. 13). When rubber was present in the blend (prior to extraction), these fiber ends must have been embedded in the rubber phase, establishing thereby fibrous bridges between the two continuous phases. These fibers help in transferring stress and can be regarded as "mechanical anchors."

Further, as a result of the particular sequence of addition of fibers to the molten thermoplastic during mixing, each fiber gets coated by the thermoplastic which is clearly evident in Figure 14. These coated fibers penetrate into the rubber phase and increase thereby the homogeneity of the blend. This contention is supported by the experimental observation of a large increase in the tear and tensile strength of the short-fiber-filled blends composed of 70 NR/30 HDPE. Here it is necessary to emphasize that these increments in the tensile properties are not solely due to the deviation of

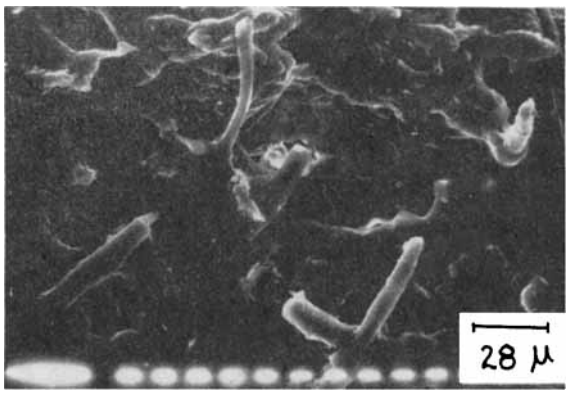

Fig. 13. SEM photomicrograph of benzene extracted surface of blend 30D (70 NR/30 HDPE/30 fiber), fiber ends sticking out of the HDPE layer.

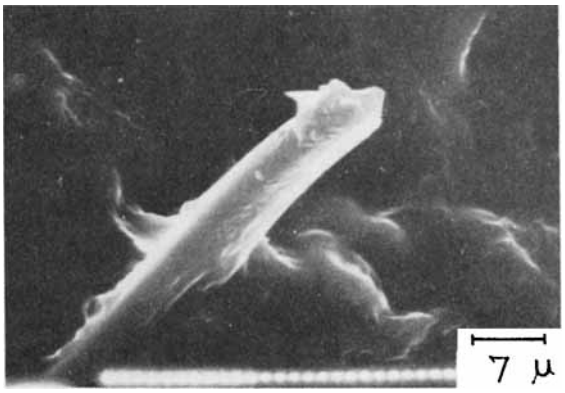

Fig. 14. SEM photomicrograph of benzene extracted surface of blend 30D: enlarged view of Figure 13; fiber is coated with the thermoplastic.

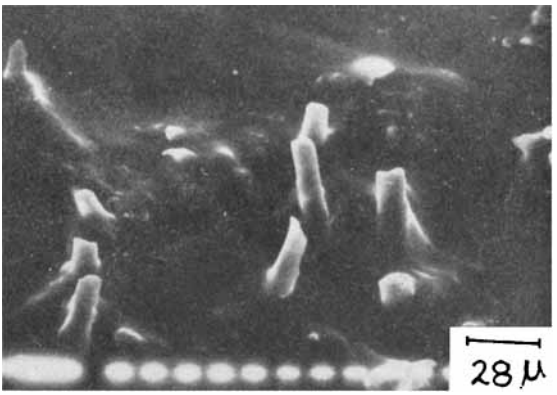

Fig. 15. SEM photomicrograph of benzene extracted surface of blend 30D with bonding system; fibers firmly embedded in the HDPE matrix.

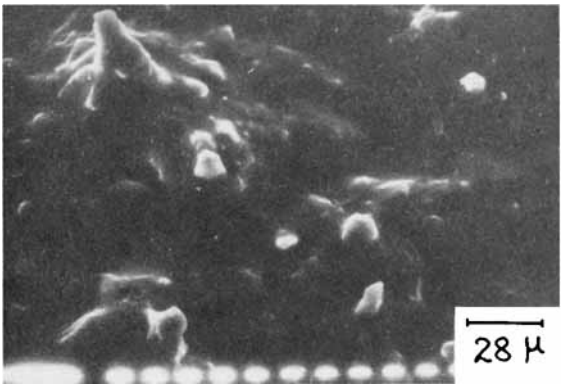

Fig. 16. SEM photomicrograph of benzene extracted surface of blend 30D with bonding system; thicker coating of the thermoplastic on the fiber and better adhesion between fiber and HDPE matrix.

the fracture path by the fibers. If that were so, other blend ratios should have shown corresponding levels of enhancement at different fiber loadings. On the contrary, owing to its particular morphology, the 70 NR/30 HDPE shows the highest increase.

Figures 15 and 16 are the photomicrographs of the surface of the NR/HDPE with 30 phr loading of short silk fiber and a bonding system composed of silica, resorcinol and hexamethylenetetramine. The bonding system gives rise to better adhesion between the fibers and the matrix. This is clearly indicated in Figures 15 and 16 by the firmly bonded fibers with a thicker coating of the plastic phase as compared to those in Figures 13 and 14. It was also noticed that the layers formed (on extraction with benzene) did not separate because of the bonding system. These observations are in conformity with the experimental observations of the effect of incorporation of a bonding system (Table VI).

PART II

Effect of Blend Ratio. Figure 17 shows the variation of tensile strength with fiber loading for different blend ratios of fiber-filled NR/LDPE composites. From the figure it is clear that the effect of the presence of fibers

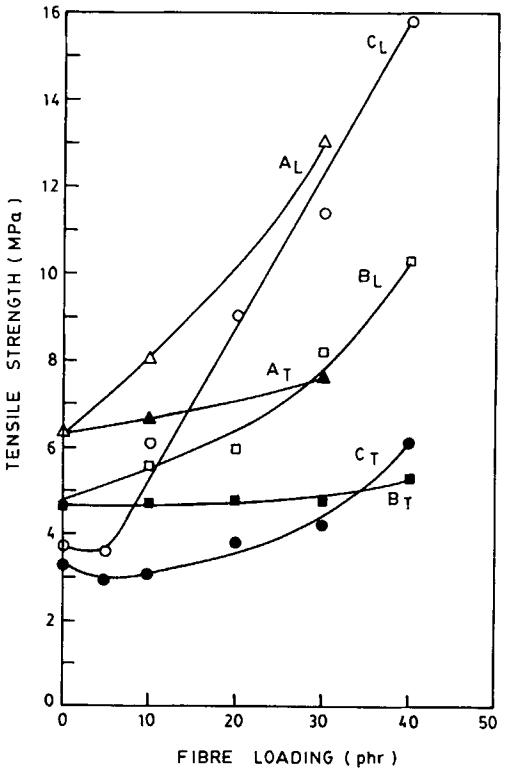

Fig. 17. Effect of fiber loading on tensile strength of NR/LDPE blends with different blend ratios.

in the mixes is more pronounced in the high rubber blends. Addition of 30 phr fiber to the high plastic blend, A, leads to an increase in the tensile strength in mixes with longitudinally oriented fibers. In the 50/50 blend, B, the addition of fibers causes an improvement in the tensile strength. In comparison to blends A and B, C shows a marked increase in the tensile strength which increases threefold at 30 phr loading of fiber. At 40 phr fiber loading the tensile strength of blend C_L exceeds those of A_L and B_L, although, at low fiber loadings, the trend is reverse. Another interesting observation is that only the high rubber mixes C_L and C_T exhibit a minimum in the tensile strength at low fiber concentrations. This phenomenon of a "critical fiber volume" has been explained earlier. The development of anisotropy as a consequence of fiber orientation in the mixes is also clearly evident from Figure 17.

Figure 18 shows the variation of elongation at break with fiber loading for various blend ratios. In all cases, the introduction of fiber leads to a drastic reduction in the ultimate elongation. Both mixes A and B become quite brittle at 30 phr loading of fiber and fiber orientation has little effect on the elongation at break in these cases. In contrast, mix C shows higher ultimate elongation values in the transverse direction as compared to that in the longitudinal, although in both cases the ultimate elongation drops sharply on the introduction of fibers.

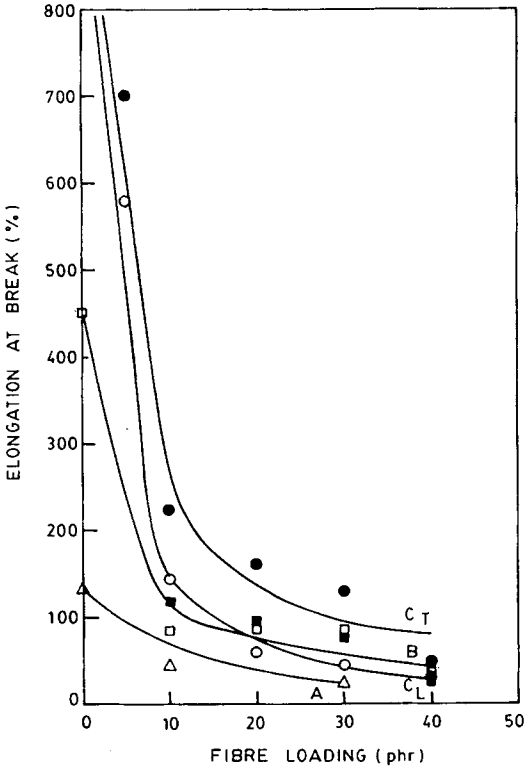

Fig. 18. Effect of fiber loading on the elongation at break of NR/LDPE blends with different blend ratios.

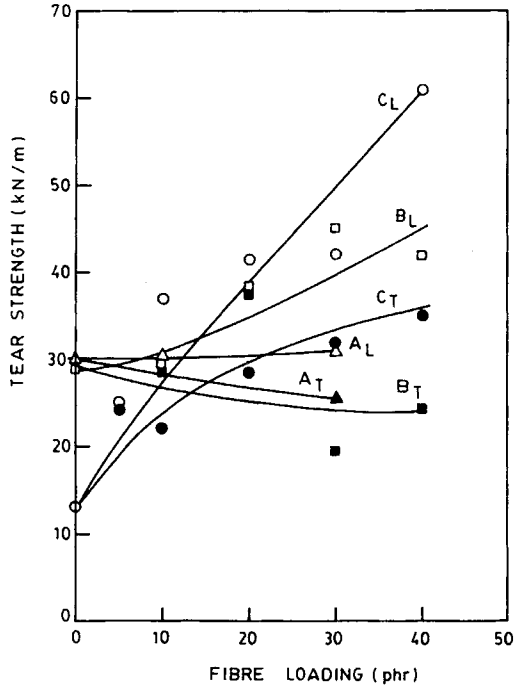

Fig. 19. Effect of fiber loading on the tear strength of NR/LDPE blends with different blend ratios.

The effect of fiber loading on the tear strength of different blend ratios is shown in Figure 19. The tear strength of the high rubber blend with longitudinal fiber orientation increases in direct proportion to the fiber loading, and at 10 phr loading of fiber its tear strength is higher than that of both

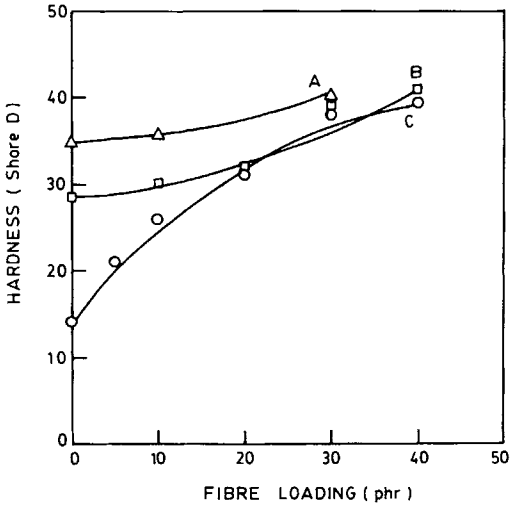

Fig. 20. Effect of fiber loading on the hardness of NR/LDPE blends with different blend ratios.

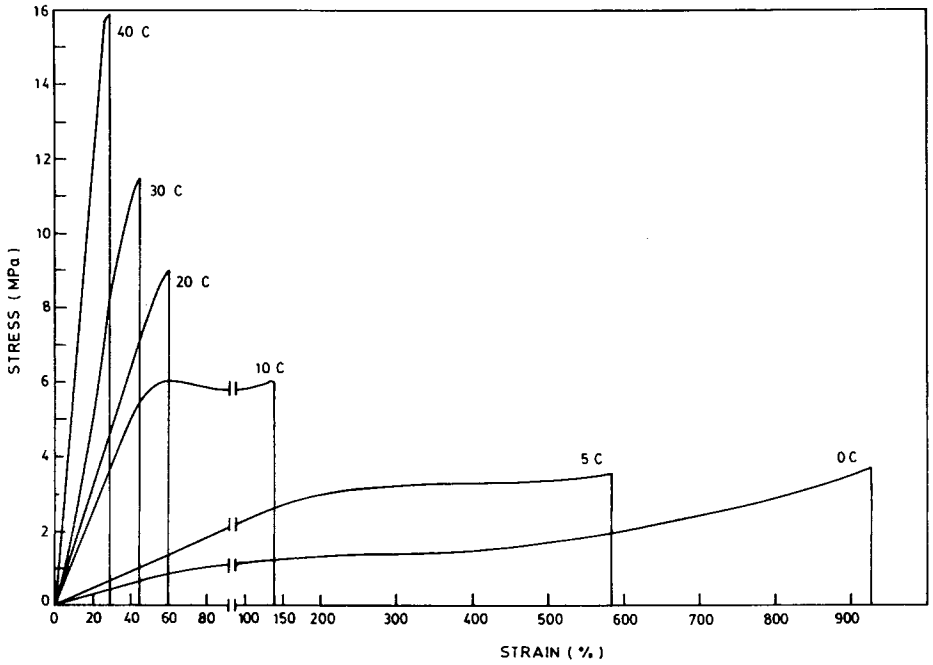

Fig. 21. Stress–strain curves of the high rubber blend C_L (70 NR/30 LDPE) with different fiber loadings.

A_L and B_L (longitudinal fiber orientation). On the other hand, B_L shows a slow increase in the tear strength while that of A_L remains essentially unchanged with increasing loading of fiber. Anisotropy in tear strength as a consequence of fiber orientation is exhibited by all blend ratios. Hardness of the blends increases with increasing fiber concentration in the mixes as shown in Figure 20. However, the hardness of the high rubber blend increases much more sharply with increasing fiber loading as compared to that of the high plastic blends. At high loadings of fiber, the hardness becomes almost constant and all the blends show similar hardness values.

Figure 21 shows the stress–strain curves of the high rubber blend C (with longitudinally oriented fibers) with different fiber loadings. When no fibers are present, C exhibits yielding, but, as the fiber volume in the mix increases, yielding decreases. Above 10 phr loading of fiber, the blends behave like elastic vulcanizates and become progressively brittle with increasing fiber loading.

SEM Studies of Fracture Surfaces

Figures 22–25 are the SEM photomicrographs of the tensile fracture surfaces of different silk-fiber-filled blends of NR and LDPE. Figures 22 and 23 are those of 50 NR/50 LDPE blends filled with 30 phr of fiber. The orientation of the fibers in the longitudinal and transverse directions, respectively, is clearly evident. The fibers appear to be well distributed over the surface. Figure 22 of $30B_L$ shows loose fiber ends sticking out of the

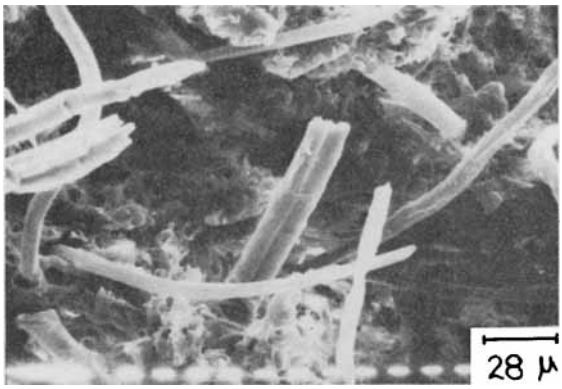

Fig. 22. SEM photomicrograph of the tensile fracture surface of blend $30B_L$; loose fiber ends sticking out of the surface.

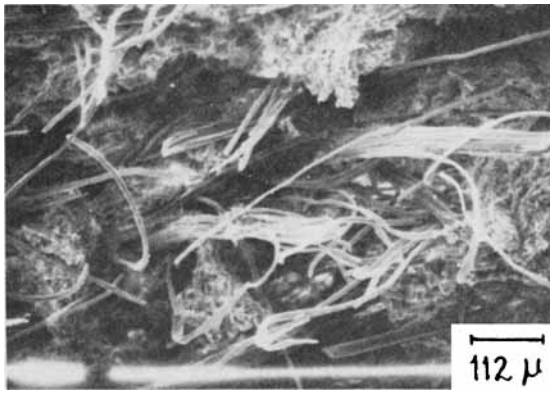

Fig. 23. SEM photomicrograph of the tensile fracture surface of blend $30B_T$; fibers embedded transversely across the surface.

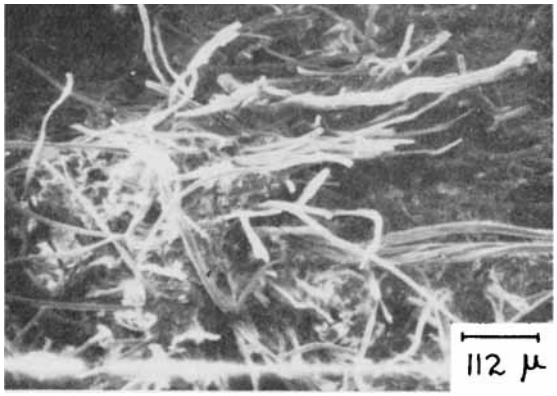

Fig. 24. SEM photomicrograph of the tensile fracture surface of blend $30C_L$; breakage and pulling out of fibers.

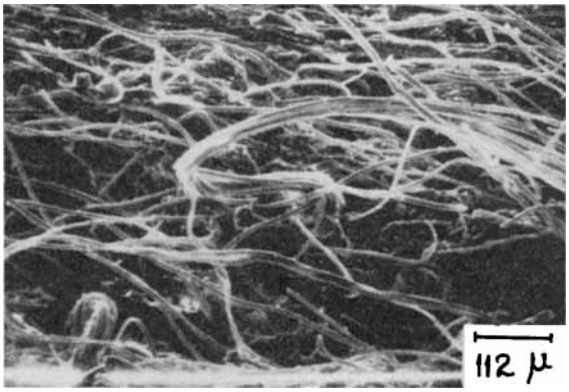

Fig. 25. SEM photomicrograph of the tensile fracture surface of blend $30C_T$; negligible breakage and pulling out of fibers.

surface unlike Figure 23 of $30B_T$ which shows fibers embedded transversely across the surface. These features are duplicated in Figures 24 and 25 which are the corresponding photomicrographs of mixes $30C_L$ and $30C_T$ (70 NR/30 LDPE/30 fiber). These characteristics can be anticipated from the study of the role of fibers during tensile fracture. The tensile strength of short-fiber-filled anisotropic mixes depends primarily on the fibers which obstruct the progress of the fracture path. Breakage and pulling out of the fibers take place when the fibers are oriented longitudinally (Fig. 1). Whereas in the case of transversely oriented fibers, the crack progresses in the direction of fiber alignment, experiencing thereby a lower resistance by the fibers and consequently fiber breakage or pulling out is insignificant.

Figures 26 and 27 are the SEM photomicrographs of the tear fracture surfaces of B_L and B_T (50:50) mixes loaded with 10 phr fiber. Both the fractographs show very similar features, which is in line with the experimental observation of similar tear strengths in both directions of fibre orientation (Fig. 19). This result implies that the volume of fibers is insufficient

Fig. 26. SEM photomicrograph of the tear fracture surface of blend $10B_L$.

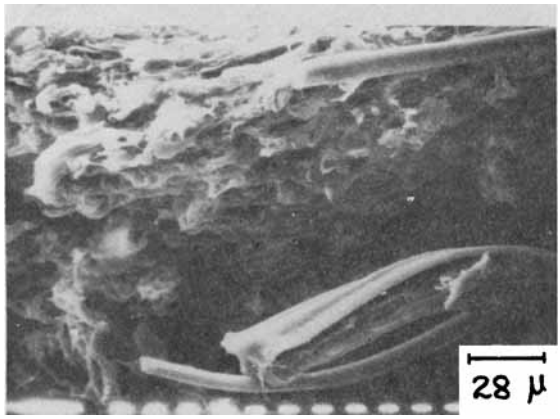

Fig. 27. SEM photomicrograph of the tear fracture surface of blend $10B_T$; features are similar to those of $10B_L$.

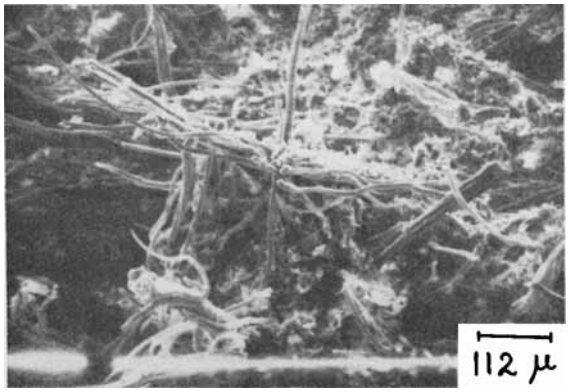

Fig. 28. SEM photomicrograph of the tear fracture surface of blend $30B_L$; loose fiber ends protruding from the surface.

Fig. 29. SEM photomicrograph of the tear fracture surface of blend $30B_T$; well-ordered bundles of fibers placed across the surface.

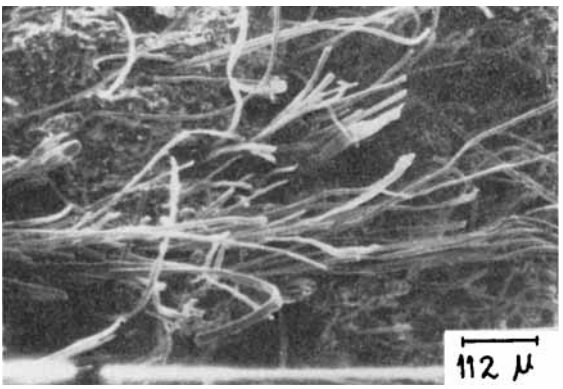

Fig. 30. SEM photomicrograph of the tear fracture surface of blend $30C_L$; features similar to that of $30B_L$ (Fig. 28).

for creating anisotropy and reinforcing the mixes. Figure 27 shows clearly (at the right-hand corner) how a layer of thermoplastic covers a strand of fiber.

Figures 28–31 are the SEM photomicrographs of the tear fracture surfaces of mixes B_L, B_T, C_L and C_T each loaded with 30 phr of fiber. In Figures 28 and 29 the phenomenon of anisotropy is clearly illustrated by the placement of the fibers in the mixes. While the mix with longitudinally oriented fibers, B_L, shows loose fiber ends, the mix with transversely oriented fibers, B_T, shows well-ordered bundles of fibers placed across the fracture surface and a total absence of loose fiber ends sticking out of the surface. It can be concluded, therefore, that the development of anisotropy in short-fiber-filled blends depends on the fiber loading among other things.

Figures 30 and 31, the tear fractographs of mixes $30C_L$ and $30C_T$, exhibit features, which are common to Figures 28 and 29 of mixes $30B_L$ and $30B_T$, respectively, i.e., loose fiber ends in the longitudinal direction of fiber orientation and an absence of the same in the transverse direction of fiber

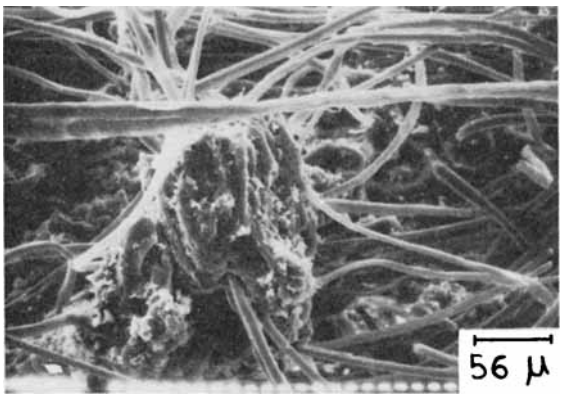

Fig. 31. SEM photomicrograph of the tear fracture surface of blend $30C_T$; features similar to that of $30B_T$ (Fig. 29), but coating with thermoplastic is comparatively less.

orientation. However, the high plastic mixes show a thicker coating of the thermoplastic on the fibers as compared to the high rubber mixes, as a result of which the fibers are stuck into bundles in the former. This observation fits in with the data of a higher thermoplastic to fiber ratio in the 50/50 blend as compared to that in the 70/30 blend because the fiber loading is based on the rubber phase only.

References

1. L. A. Goettler and K. S. Shen, *Rubber Chem. Technol.*, **56**, 619 (1983).
2. S. R. Moghe, *Rubber Chem. Technol.*, **49**, 1160 (1976).
3. J. E. O'Connor, *Rubber Chem. Technol.*, **50**, 945 (1977).
4. V. M. Murthy and S. K. De, *J. Appl. Polym. Sci.*, **29**, 1355 (1984).
5. V. M. Murthy and S. K. De, *Rubber Chem. Technol.*, **55**, 287 (1982).
6. M. L. Kerber, T. P. Kravchenko, and N. Ya. Valetskaya, *Int. Polym. Sci. Technol.*, **8**(6), T/10 (1981).
7. J. L. Kardos, *Critical Rev. Solid State Sci.*, **3**(4), 419 (1973).
8. M. Miwa, A. Nakayama, T. Ohsawa, and A. Hasegawa, *J. Appl. Polym. Sci.*, **23**, 2957 (1979).
9. D. B. Eagles, B. F. Blumentritt, and S. L. Cooper, *J. Appl. Polym. Sci.*, **20**, 435 (1976).
10. B. Harris, P. W. R. Beaumont, and E. Moncunill deFerran, *J. Mater. Sci.*, **6**, 238 (1971).
11. M. J. Folkes, *Short Fibre Reinforced Thermoplastics*, Wiley, Chichester, 1982.
12. S. Akhtar, P. P. De, and S. K. De, *Mater. Chem. Phys.*, **12**, 235 (1985).
13. D. K. Setua and S. K. De, *Rubber Chem. Technol.*, **56**, 808 (1983).
14. D. K. Setua and S. K. De, *J. Mater. Sci.*, **19**, 983 (1984).
15. D. K. Setua and B. Dutta, *J. Appl. Polym. Sci.*, **29**, 3097 (1984).
16. D. D. Dunnom, *Rubber Age*, **100**, 49 (1968).
17. L. H. Lee, *J. Polym. Sci.*, **5**, 751 (1967).
18. N. L. Hewitt, *Rubber Age*, **104**, 59 (1972).
19. S. R. Moghe, *Rubber Chem. Technol.*, **47**, 1074 (1974).
20. J. M. Campbell, *Prog. Rubber Technol.*, **41**, 43 (1978).
21. K. Boustany and P. Hamed, *Rubber World*, **171**(2), 39 (1974).

Received September 17, 1985
Accepted November 6, 1985